In vivo internal tumor illumination by telomerase-dependent adenoviral GFP for precise surgical navigation

Hiroyuki Kishimoto[a,b,c], Ming Zhao[a], Katsuhiro Hayashi[a,b], Yasuo Urata[d], Noriaki Tanaka[c], Toshiyoshi Fujiwara[c,e], Sheldon Penman[f,1], and Robert M. Hoffman[a,b,1]

[a]AntiCancer, Inc., San Diego, CA 92111; [b]Department of Surgery, University of California, San Diego, CA 92103-8220; [c]Division of Surgical Oncology, Department of Surgery, Okayama University Graduate School of Medicine, Dentistry and Pharmaceutical Sciences, Okayama 700-8558, Japan; [d]Oncolys BioPharma, Inc., Tokyo 106-0032, Japan; [e]Center for Gene and Cell Therapy, Okayama University Hospital, Okayama 700-8558, Japan; and [f]Department of Biology, Massachusetts Institute of Technology, Cambridge, MA 02139-4307

Contributed by Sheldon Penman, June 8, 2009 (sent for review May 10, 2009)

Cancer surgery requires the complete and precise identification of malignant tissue margins including the smallest disseminated lesions. Internal green fluorescent protein (GFP) fluorescence can intensely illuminate even single cells but requires *GFP* sequence transcription within the cell. Introducing and selectively activating the *GFP* gene in malignant tissue in vivo is made possible by the development of OBP-401, a telomerase-dependent, replication-competent adenovirus expressing GFP. This potentially powerful adjunct to surgical navigation was demonstrated in 2 nude mouse models that represent difficult surgical challenges—the resection of widely disseminated cancer. HCT-116, a model of intraperitoneal disseminated human colon cancer, was labeled by virus injection into the peritoneal cavity. A549, a model of pleural dissemination of human lung cancer, was labeled by virus administered into the pleural cavity. Only the malignant tissue fluoresced brightly in both models. In the intraperitoneal model of disseminated cancer, fluorescence-guided surgery enabled resection of all tumor nodules labeled with GFP by OBP-401. The data in this report suggest that adenoviral-GFP labeling tumors in patients can enable fluorescence-guided surgical navigation.

Adenovirus | green fluorescent protein | metastasis

The intent of cancer surgery is to remove malignant tissue together with margins of presumably normal tissue (1–3) to ensure complete removal of abnormal cells. Estimating margin width during surgery is critical and depends on the surgeon's vision. There have been many developments intended to improve the delineation of tissue margins using morphologic and optical differences between normal and abnormal tissue. This report describes a major enhancement of cancer surgical navigation using the selective fluorescent labeling, in vivo, of malignant tissue. Bright GFP fluorescence clearly illuminates the tumor boundaries and facilitates detection of the smallest disseminated disease lesions.

Highly selective viral replication in malignant cells growing in normal tissue has recently become possible using novel adenoviruses, OBP-301 (4–6) and, more recently, OBP-401 (7, 8). This latter virus, which can enter most cells, contains the replication cassette with the human telomerase reverse transcriptase (hTERT) promoter driving the expression of the viral *E1* genes, and the inserted *GFP* gene. Virus replication and, hence, *GFP* gene expression occur only in the presence of an active telomerase, i.e., in malignant tissue (7). The OBP-401 virus was first tested by injection directly into HT-29 human colon tumors orthotopically implanted into the rectum in BALB/c *nu*/*nu* mice (7). Subsequent para-aortic lymph node metastasis was observed by laparotomy under fluorescence. The adaption of GFP fluorescence to in vivo labeling of tumor tissue should facilitate precision surgical navigation in live animals and, very possibly, in a clinical surgical setting.

Results

Fluorescence Labeling of Human Cancer Cells with OBP-401 in Vitro. A549 tumor cells, growing in tissue culture, were infected with OPP-401, and the development of GFP fluorescence followed. The fluorescence intensity gradually increased after infection as the virus, with its *GFP* gene, replicated (Fig. 1*A*).

The extent of infection was tested by infecting red fluorescent protein (RFP)-expressing cancer cells, growing in cell culture, with OBP-401. These included A549-RFP, PC-3-RFP, HCT-116-RFP, and HT-29-RFP cells. In most cells, the introduction of green fluorescence changes the cell color from red to yellow, showing that most were infected by OBP-401. Any remaining red fluorescence clearly identifies those few cells that remain uninfected by the adenovirus. The color changes increased gradually followed by cell death due to the cytopathic effect of replicating OBP-401 (Fig. 1 *B* and *C*).

Fluorescence Labeling of Subcutaneous Tumors by Infection in Vivo with OBP-401. Both nonfluorescent PC-3 and red fluorescent PC-3-RFP human prostate cancer cells were inoculated s.c. (Fig. 2 *A* and *B*). The resulting s.c. tumors were injected with 1×10^8 plaque-forming units (PFU) of OBP-401 as shown in Fig. 2*B*. A color change from red to yellow in the s.c. PC-3-RFP tumor and the onset of GFP fluorescence in the nonfluorescent PC-3 tumor were observed by the third day after virus injection (Fig. 2*C*). An RFP filter selectively showed the tumors' endogenous RFP fluorescence (Fig. 2*D*). Similarly, a GFP filter showed GFP fluorescence induced in the tumors by OBP-401 (Fig. 2*E*). Infecting tumor cells that are endogenously expressing RFP with the GFP-expressing adenoviral vector OBP-401 clearly shows the extent of GFP labeling of the tumor. Cells showing a yellow fluorescence are infected with OBP-401, while the remaining red fluorescent cells clearly indicate the small portion that might remain uninfected.

Labeling Peritoneal Carcinomatosis with OBP-401. Peritoneal carcinomatosis was induced in the abdominal cavity of nude mice by inoculating 3×10^6 red fluorescent HCT-116-RFP human colorectal cancer cells. Various sized peritoneal disseminated nodules developed within 12 days. These were clearly visible by fluorescence imaging using a long-pass filter and/or a specific RFP filter (Fig. 3 *A* and *B*). Even very small disseminated nodules were illuminated by RFP fluorescence (Fig. 3*B*). Although there was some autofluorescence from adjacent organs visible, the tumor nodules were not visible through a GFP filter (Fig. 3 *A* and *B*).

Author contributions: H.K., Y.U., N.T., T.F., and R.M.H. designed research; H.K., M.Z., and K.H. performed research; H.K., Y.U., N.T., T.F., S.P., and R.M.H. analyzed data; and H.K., S.P., and R.M.H. wrote the paper.

The authors declare no conflict of interest.

[1]To whom correspondence may be addressed. E-mail: penman@mit.edu or all@anticancer.com.

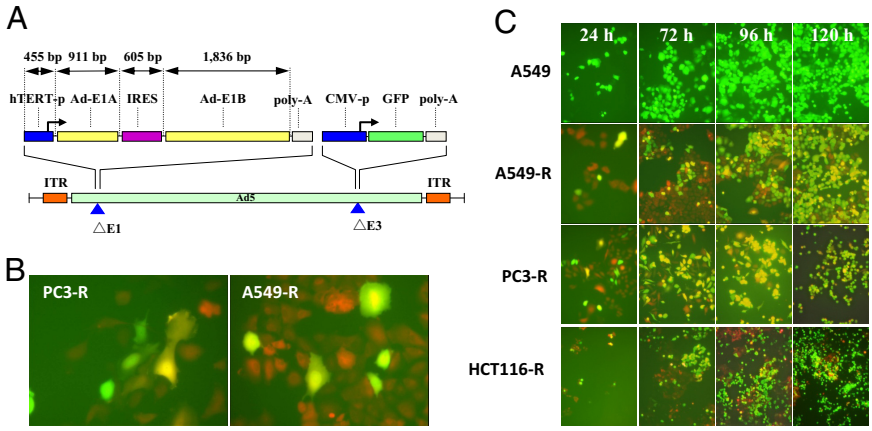

Fig. 1. Structure of OBP-401, virus replication in human cancer cells and induced GFP expression. (*A*) Schematic DNA structure of OBP-401. OBP-401 is a telomerase-specific replication-competent adenovirus variant, in which the hTERT promoter element drives the expression of *E1A* and *E1B* genes linked with an IRES. The *GFP* gene is inserted under the CMV promoter into the E3 region. (*B*) A549-RFP and PC-3-RFP cells changed color after infection with OBP-401 at a multiplicity of injection (MOI) of 10. (Magnification, 200×.) (*C*) Noncolored A549 as well as RFP-expressing cancer cells A549-RFP, PC-3-RFP, and HCT-116-RFP were infected with OBP-401 at an MOI of 10. Cells were assessed at indicated time points for GFP expression under fluorescence microscopy. After OBP-401 infection, noncolored A549 cells expressed GFP fluorescence. In A549-RFP, PC-3-RFP, and HCT-116-RFP, color changes from red to yellow were detected. The color changes increased gradually in a time-dependent fashion. (Magnification, 200×.)

Once the malignant nodules were established at 12 days after intraperitoneal (i.p.) implantation of HCT-116-RFP cells, 1×10^8 PFU OBP-401 were injected into the mouse abdominal cavity. Selective color filters showed that the HCT-116-RFP disseminated nodules expressed GFP fluorescence as well as RFP when examined 5 days later (Fig. 3*C*). RFP fluorescence

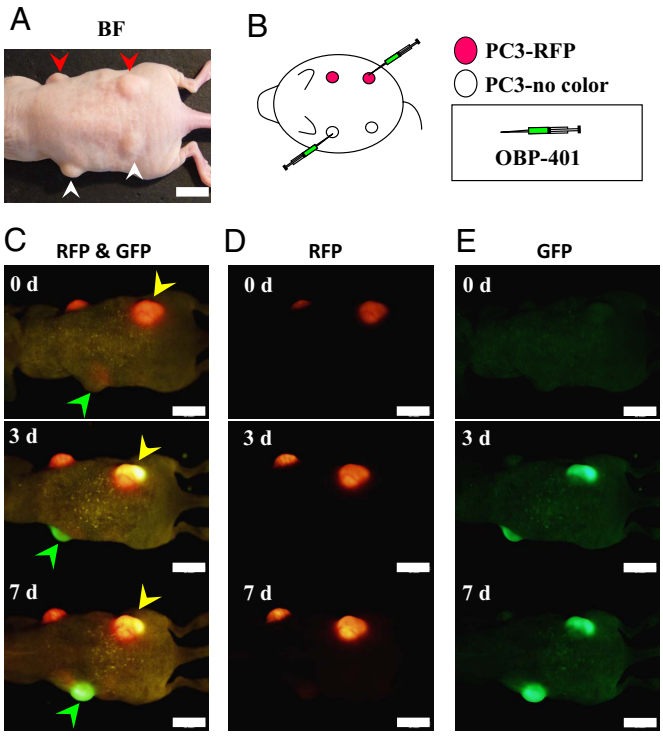

Fig. 2. Selective visualization of s.c. tumors in vivo after OBP-401 GFP-labeling. s.c. tumors of noncolored PC-3 (*A*, white arrowheads) or PC-3-RFP (*A*, red arrowheads) human prostate cancer cells were intratumorally injected with PBS for control or OBP-401 at a dose of 1×10^8 PFU as shown in *B*. After intratumoral injection of OBP-401, GFP fluorescence was detected in noncolored PC-3 s.c. tumors (*C*, green arrowheads) and a color change from red to yellow was also observed in PC-3-RFP tumors by fluorescence imaging using a long-pass filter to simultaneously observe both GFP and RFP (*C*, yellow arrowheads). With specific filters, the tumors endogenous RFP fluorescence (*D*) and GFP fluorescence induced by OBP-401 (*E*) were individually detected. (Scale bar, 10 mm.)

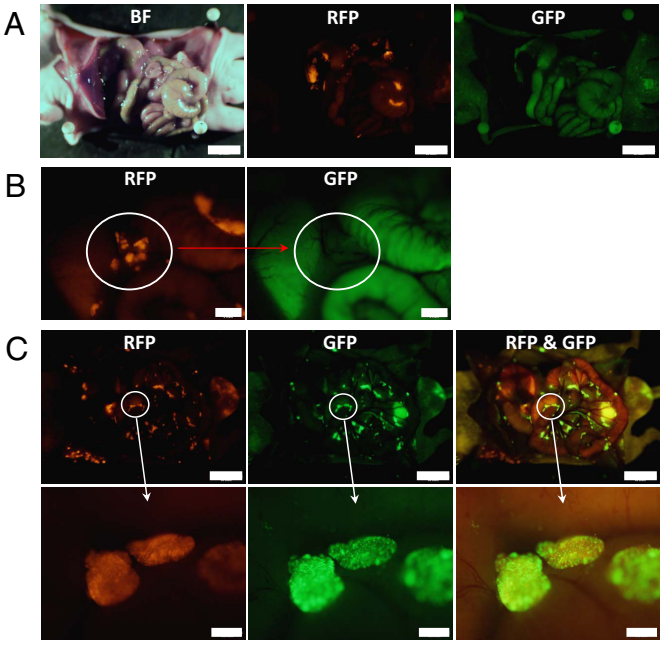

Fig. 3. Intraperitoneal injection of OBP-401 visualized peritoneal dissemination of HCT-116-RFP cells. (*A*) HCT-116-RFP human colorectal cancer cells were inoculated into the abdominal cavity of nude mice. Various sized disseminated peritoneal nodules appeared within 12 days. (Scale bar, 10 mm.) (*B*) At higher magnification, peritoneally disseminated nodules of HCT-116-RFP were clearly visible using a specific filter for RFP (*Left*), and these nodules did not express GFP (*Right*). (Scale bar, 2 mm.) (*C*) Mice with HCT-116-RFP peritoneal disseminated nodules were i.p. injected with OBP-401 at a dose of 1×10^8 PFU. Five days after virus administration, HCT-116-RFP peritoneal-disseminated nodules were detected with their endogenous RFP fluorescence (*Left*). These disseminated nodules now expressed GFP fluorescence (*Middle*). With the long-pass filter, for simultaneous observation of both GFP and RFP, it can be seen that all of the RFP tumors were apparently labeled with GFP after OBP-401 injection (*Right*). (Scale bars: *Upper*, 10 mm; *Lower*, 500 μm.)

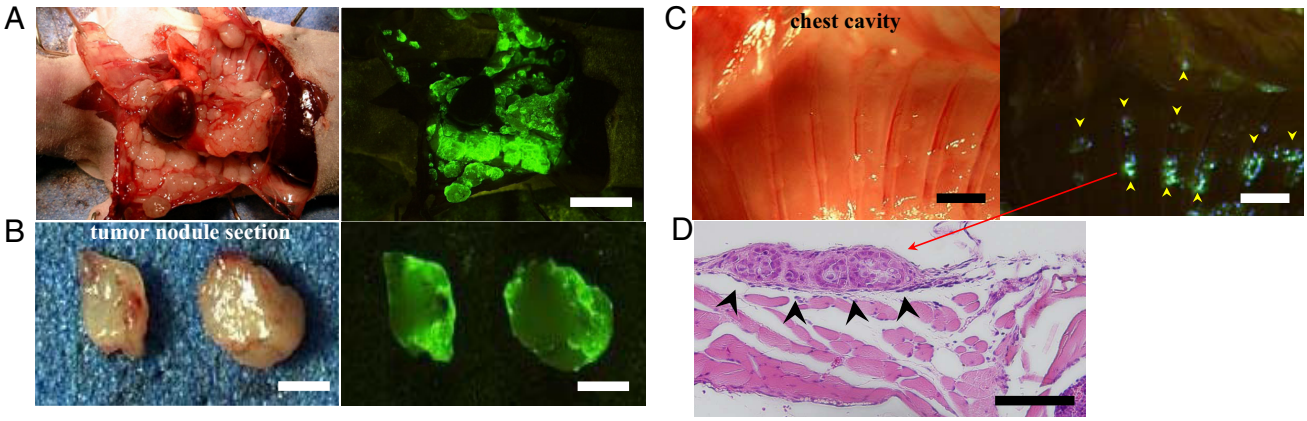

Fig. 4. Intrapleural injection of OBP-401 visualized pleural disseminations of A549 cells. (*A*) Two weeks after implantation of noncolored A549 cells into the thoracic space, OBP-401 at a dose of 1×10^8 PFU, was intrapleurally injected. Five days later, disseminated nodules were visualized by GFP fluorescence (*Right*). (Scale bar, 10 mm.) (*B*) Cross-section of pleural disseminated nodule. GFP expression was seen on the surface of pleurally disseminated nodules (*Right*). (Scale bar, 2 mm.) (*C*) Very small lesions that were not detectable in brightfield were visualized by GFP fluorescence (*Right*, arrowheads). (Scale bar, 2 mm.) (*D*) Histological analysis with H&E confirmed that these GFP-expressing lesions were adenocarcinomas (arrowheads). (Scale bar, 100 μm.)

was essentially coincident with that of GFP (Fig. 3*C*). These results indicate that i.p. injection of OBP-401 efficiently infected and labeled disseminated cancer.

Labeling of Pleurally Disseminated Cancer with OBP-401. These experiments assessed the effectiveness of OBP-401 labeling of pleural carcinomatosis in a mouse model of unlabeled A549 human lung cancer cells. The thoracic space of nude mice was inoculated with 2×10^6 cancer cells. Various sized disseminated plural nodules appeared within 10 days after implantation. At this time, 1×10^8 PFU of OBP-401 were injected into the thoracic cavity. Five days after injection of OBP-401, the cavity was examined using GFP fluorescence imaging. A representative mouse is shown in Fig. 4. Disseminated pleural nodules were visualized by GFP expression (Fig. 4 *A* and *B*). Even very small lesions, which are normally undetectable, were clearly illuminated by GFP fluorescence (Fig. 4*C*). Histological examination confirmed that these GFP-expressing tissues were adenocarcinomas. A representative histological section is shown in Fig. 4*D*. These results suggest that intrapleural injection of at least 1×10^8 PFU of OBP-401 can efficiently label disseminated pleural cancer. Lower doses of OBP-401 resulted in less efficient labeling.

OBP-401 Fluorescence-Guided Resection of Disseminated Peritoneal Tumors. In order to test the effectiveness of OBP-401-guided cytoreduction surgery, we used the peritoneal carcinomatosis model with nonfluorescent HCT-116 human colon cancer cells. Mice with peritoneal carcinomatosis were injected i.p. with OBP-401 at a dose of 1×10^8 PFU. Five days after viral administration, laparotomy was performed to remove intra-abdominal disease using fluorescence-guided navigation under anesthesia (Fig. 5 *A* and *B*). A representative mouse after cytoreduction surgery with OBP-401-navigation is shown in Fig. 5*C*. Disseminated cancer nodules, which would otherwise be undetectable, were clearly visible by bright GFP fluorescence. The resected nodules were visualized as frozen sections under both fluorescence (Fig. 5*D*) and after hematoxylin and eosin (H&E) staining (Fig. 5 *E* and *F*). These results suggest that OBP-401-labeling has significant potential for guiding cytoreduction surgery of disseminated cancer.

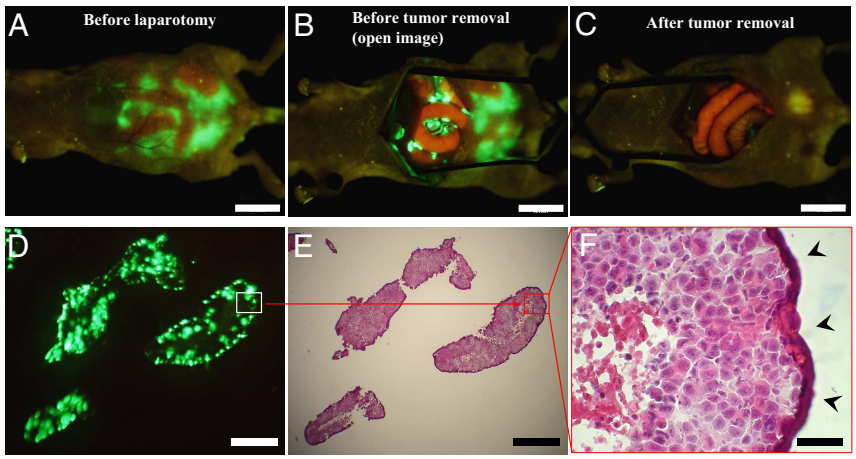

Fig. 5. Fluorescence-guided surgical removal of peritoneal disseminated HCT-116 tumors after GFP labeling with OBP-401. Noncolored HCT-116 human colon cancer cells were injected into the abdominal space of nude mice. Ten days later, 1×10^8 PFU of OBP-401 were i.p. injected. (*A*) Disseminated nodules were efficiently labeled and noninvasively visualized by GFP expression 5 days after virus administration. (*B*) Under general anesthesia, laparotomy was performed to remove intra-abdominal disease under GFP-guided navigation. (*C*) Disseminated nodules visualized by GFP-guided navigation were removed. (Scale bars: *A*–*C*, 10 mm.) (*D*) Frozen section of resected HCT-116 disseminated nodules with fluorescence detection. (Scale bar, 500 μm.) (*E*) H&E section of HCT-116 disseminated nodules shown in *D*. The box outlines a region of *D* and *E* analyzed in *F*. (Scale bar, 500 μm.) (*F*) Detail of the boxed region of *D* and *E*. (Scale bar, 50 μm.)

Discussion

The peritoneal surface is involved in more than 20% of patients with gastric, colon, and pancreatic cancers (1). Cytoreduction surgery requires resection of all visible tumors and stripping of all peritoneal surfaces that contain metastatic nodules (1, 2, 9). Therefore, visceral peritoneal involvement often requires concomitant resection of intra-abdominal organs such as the small intestine and colorectum.

The detection of small macroscopic peritoneal lesions is largely limited by the weak contrast between tumor nodules and surrounding normal tissues. Technology improving the intraoperative detection of peritoneal disease would facilitate essentially complete cytoreduction in these patients. The photosensitizer, 5-aminolevulinic acid (5-ALA) has been used for intraoperative detection of cancer lesions in neurosurgery (10). However, labeling that is essentially cancer-selective can be a powerful surgical adjunct. This report shows that OBP-401 infection of cancer cells leads to the highly selective induction of bright GFP fluorescence.

Implanting RFP-expressing cancer cell lines gave rise to fluorescent nodules whose color change clearly indicated the efficiency with which OBP-401 labeled disseminated peritoneal tumors with GFP. The change from red to yellow fluorescence indicated successful infection by OBP-401 (Fig. 3). Similarly, OBP-401 GFP labeling could detect dissemination nodules with high sensitivity in a pleural carcinomatosis model (Fig. 4).

Perhaps most importantly, we could remove disseminated disease in a peritoneal carcinomatosis model by using fluorescence-guided resection. These results suggest developing a dedicated excitation light for fluorescence-guided surgery similar to that described for use in mice (11). In the present study, during surgery, even very small peritoneal lesions could be identified with GFP fluorescence (11).

Materials and Methods

Recombinant Adenovirus. OBP-401, containing the *GFP* gene under the control of the CMV promoter with the hTERT promoter driving the *E1A* and *E1B* genes, was constructed as previously described (6, 7). OBP-401 was purified by ultracentrifugation in cesium chloride step gradients. Virus titers were determined by a plaque-forming assay using 293 cells. The virus was stored at −80°C.

Cell Culture. The human non-small cell lung cancer cell line A549, the human colorectal cancer cell lines HCT-116 and HT-29, and the human prostate cancer cell line PC-3 were cultured in RPMI 1640 medium supplemented with 10% FBS.

Production of RFP Retroviral Vector. For RFP retrovirus production, the *Hind*III/*Not*I fragment from pDsRed2 (Clontech), containing the full-length RFP cDNA, was inserted into the *Hind*III/*Not*I site of pLNCX2 (Clontech) containing the neomycin-resistance gene. PT67, a NIH 3T3-derived packaging cell line (Clontech), expressing the viral envelope, was cultured in DMEM supplemented with 10% FBS. For vector production, PT67 packaging cells, at 70% confluence, were incubated with a precipitated mixture of LipofectAMINE reagent (Life Technologies) and saturating amounts of pLNCX2-DsRed2 plasmid for 18 h. Fresh medium was replenished at this time. The cells were examined by fluorescence microscopy 48 h post-transduction. For selection of a clone producing high amounts of RFP retroviral vector (PT67-DsRed2), the cells were cultured in the presence of 200 to 1,000 μg/mL G418 (Life Technologies) for 7 d. The isolated packaging cell clone was termed PT67-DsRed2 (12–15).

***RFP* Gene Transduction of Cancer Cells.** For *RFP* gene transduction, cancer cells were incubated with a 1:1 precipitated mixture of retroviral supernatants of PT67-DsRed2 cells and RPMI 1640 containing 10% FBS for 72 h. Fresh medium was replenished at this time. Tumor cells were harvested with trypsin/EDTA 72 h post-transduction and subcultured at a ratio of 1:15 into selective medium, which contained 200 μg/mL G418. To select brightly fluorescent cells, the level of G418 was increased up to 800 μg/mL in a stepwise manner. RFP-expressing cancer cells were isolated with cloning cylinders (Bel-Art Products) using trypsin/EDTA. Cells were amplified by conventional culture methods in the absence of selective agent (12–15).

Animal Experiments. Athymic nude mice were kept in a barrier facility under HEPA filtration. Mice were fed with autoclaved laboratory rodent diet (Tecklad LM-485, Western Research Products). All animal studies were conducted in accordance with the principals and procedures outlined in the National Institutes of Health Guide for the Care and Use of Laboratory Animals under assurance A3873–01.

Subcutaneous Tumor Model. Subcutaneous tumors were produced by injection of 3×10^6 noncolored PC-3 or PC-3-RFP human prostate cancer cells in 5-week old nude mice. When tumors reached approximately 6 mm in diameter, the tumors were intratumorally injected with PBS for control or OBP-401 at a dose of 1×10^8 PFU in 100 μL PBS. Mice were examined for fluorescence expression with a long-pass filter (a filter for simultaneous observation of both GFP and RFP) or with specific filters for GFP or RFP.

Peritoneal Carcinomatosis Model of HCT-116 Human Colon Cancer Cells. Five-week-old nude mice were i.p. injected with noncolored HCT-116 or HCT-116-RFP human colon cancer cells (3×10^6 in 200 μL HBSS) using a 27-gauge needle. Twelve days after cancer cell inoculation, mice were injected i.p. with OBP-401 at a dose of 1×10^8 PFU in 200 μL PBS. Five days after virus injection, the abdominal cavity was directly examined by fluorescence imaging under anesthesia.

Pleural Carcinomatosis Model of A549 Human Lung Cancer Cells. Five-week-old nude mice were inoculated with noncolored A549 cells (2×10^6 cells in 200 μL HBSS) into the thoracic space using a 27-gauge needle. Ten days after cancer cell inoculation, OBP-401 at a dose of 1×10^8 PFU in 200 μL PBS was intrapleurally injected. Five days after virus injection, the pleural cavity was directly imaged for GFP expression. GFP-expressing tissues were removed and examined microscopically.

Fluorescence Optical Imaging and Processing. An Olympus OV100 Small Animal Imaging System containing an MT-20 light source was used. High-resolution images were captured directly on a PC (Fujitsu Siemens). Images were analyzed with the use of Cell^R software (Olympus Biosystems) (16).

Histological Examination. For histological studies, GFP-expressing tissues were removed at the time of sacrifice and put into buffered formalin for 24 h at room temperature. All of the tissues were subsequently processed through alcohol dehydration and paraffinization. Tissues were embedded in paraffin and sectioned at 5 μm. All slides were stained by H&E, and examined microscopically.

ACKNOWLEDGMENTS. This project was supported in part by National Cancer Institute Grant CA132242.

1. Sugarbaker PH (2004) Managing the peritoneal surface component of gastrointestinal cancer. Part 1. Patterns of dissemination and treatment options. *Oncology* 18:51–59.
2. Sugarbaker PH (2004) Managing the peritoneal surface component of gastrointestinal cancer. Part 2. Perioperative intraperitoneal chemotherapy. *Oncology* 18:207–219.
3. Glehen O, et al. (2004) Cytoreductive surgery combined with perioperative intraperitoneal chemotherapy for the management of peritoneal carcinomatosis from colorectal cancer: A multi-institutional study. *J Clin Oncol* 22:3284–3292.
4. Kawashima T, et al. (2004) Telomerase-specific replication-selective virotherapy for human cancer. *Clin Cancer Res* 10:285–292.
5. Taki M, et al. (2005) Enhanced oncolysis by a tropism-modified telomerase-specific replication-selective adenoviral agent OBP-405 ('Telomelysin-RGD'). *Oncogene* 24:3130–3140.
6. Umeoka T, et al. (2004) Visualization of intrathoracically disseminated solid tumors in mice with optical imaging by telomerase-specific amplification of a transferred green fluorescent protein gene. *Cancer Res* 64:6259–6265.
7. Kishimoto H, et al. (2006) In vivo imaging of lymph node metastasis with telomerase-specific replication-selective adenovirus. *Nat Med* 12:1213–1219.
8. Fujiwara T, et al. (2006) Enhanced antitumor efficacy of telomerase-selective oncolytic adenoviral agent OBP-401 with docetaxel: Preclinical evaluation of chemovirotherapy. *Int J Cancer* 119:432–440.
9. Sadeghi B, et al. (2000) Peritoneal carcinomatosis from non-gynecologic malignancies: Results of the EVOCAPE 1 multicentric prospective study. *Cancer* 88:358–363.
10. Stepp H, et al. (2007) ALA and malignant glioma: Fluorescence-guided resection and photodynamic treatment. *J Environ Pathol Toxicol Oncol* 26:157–164.
11. Yang M, Luiken G, Baranov E, Hoffman RM (2005) Facile whole-body imaging of internal fluorescent tumors in mice with an LED flashlight. *Biotechniques* 39:170–172.
12. Hoffman RM (2005) The multiple uses of fluorescent proteins to visualize cancer in vivo. *Nat Rev Cancer* 5:796–806.
13. Hoffman RM, Yang M (2006) Subcellular imaging in the live mouse. *Nature Protoc* 1:775–782.
14. Hoffman RM, Yang M (2006) Color-coded fluorescence imaging of tumor-host interactions. *Nature Protoc* 1:928–935.
15. Hoffman RM, Yang M (2006) Whole-body imaging with fluorescent proteins. *Nature Protoc* 1:1429–1438.
16. Yamauchi K, et al. (2006) Development of real-time subcellular dynamic multicolor imaging of cancer-cell trafficking in live mice with a variable-magnification whole-mouse imaging system. *Cancer Res* 66:4208–4214.